CHAPTER V

COUPLING BETWEEN NEMATIC AND SMECTIC ORDERING IN THE REENTRANT NEMATIC SYSTEMS

5.1. INTRODUCTION

The analogy between the smectic A liquid crystal and the superconducting phase of metals is now well known.[1,2] They both possess a special feature in that their order parameters are coupled to "gauged fields" (vector potential for the superconductor and the director for the smectic A liquid crystal) whose fluctuations diverge at long wavelengths. Halperin, Lubensky and Ma[3] have argued that the superconducting phase transition should be weakly first-order because of the effects of fluctuations in the intrinsic magnetic field. From a similar argument Halperin and Lubensky[4] have shown that the "critical properties" of a smectic A liquid crystal are isomorphic to those of a superconductor so much so that the smectic A-nematic transition is always

expected to be weakly first order due to coupling between smectic ordering and nematic director fluctuations. However, this has not been conclusively established experimentally so far.

The influence of smectic ordering on the thermodynamic properties of the nematic-isotropic transition has been demonstrated by a number of experiments. Achard et al.[5] investigated the temperature-concentration diagrams of systems exhibiting a nematic-smectic A-smectic C (NAC) point and cholesteric (N*)-smectic A-smectic C* (N*AC*) point. They found an interesting result that the entropy associated with N-I transition when plotted as a function of concentration (X), shows a singularity, the maximum of the singularity occurring exactiy at the concentration for which NAC or N*AC* point occurs (see figures 5.1 and 5.2). The conclusion was therefore drawn that the coupling between smectic and nematic ordering is influencing the thermodynamic behaviour of N-I transition. Shashidhar et al.[6] and Kleinhans et al.[7,8] have studied the effect of pressure on N-I transition in mixtures of 4'-n-hexyloxy-4-cyanobiphenyl and

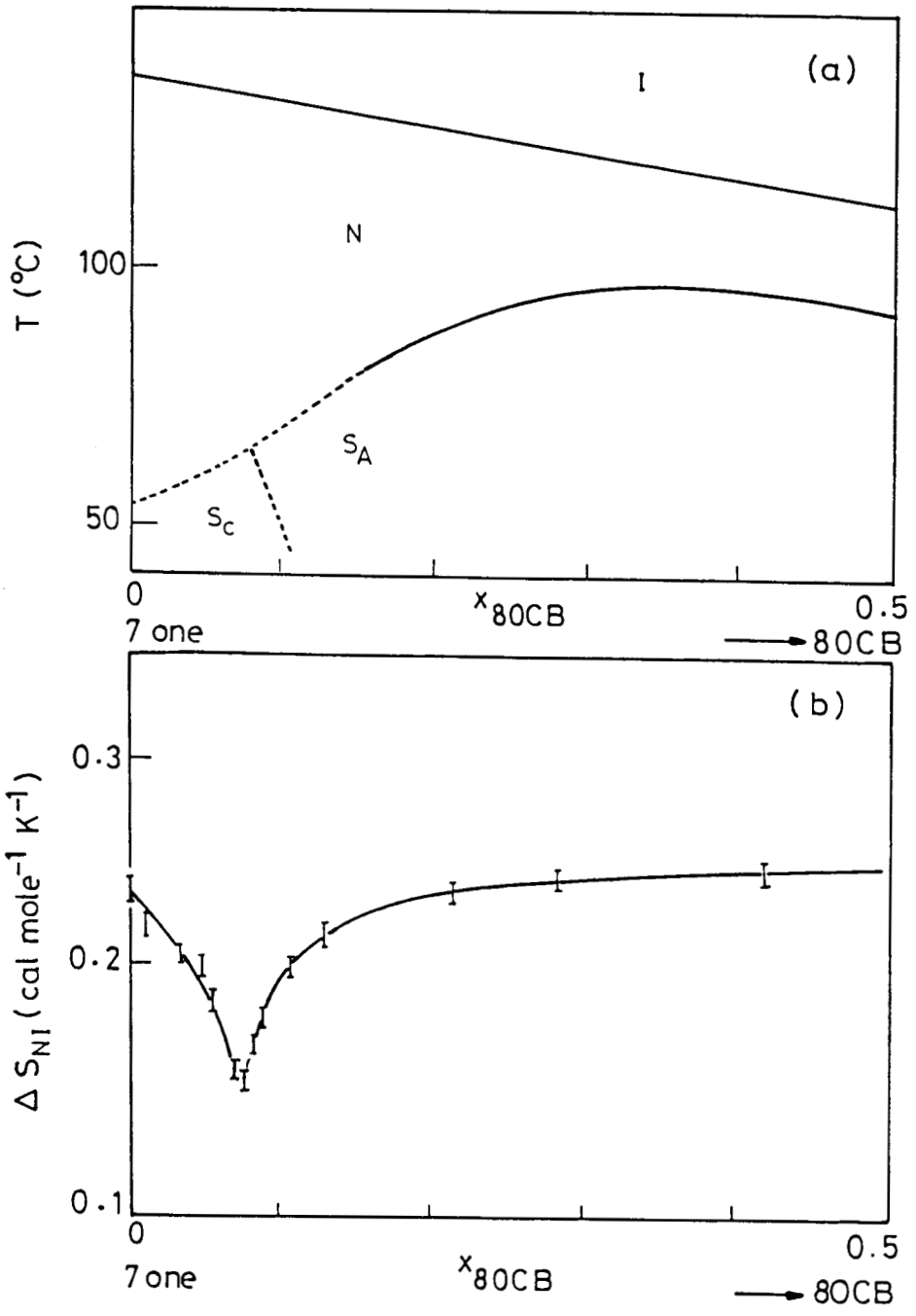

Figure 5.1

a) Binary isobaric (1 bar) diagram between 7ONE and 8OCB.

b) Variation of the nematic-isotropic transition entropy versus the molar fraction of 80CB in mixture with 7ONE (Ref. 5).

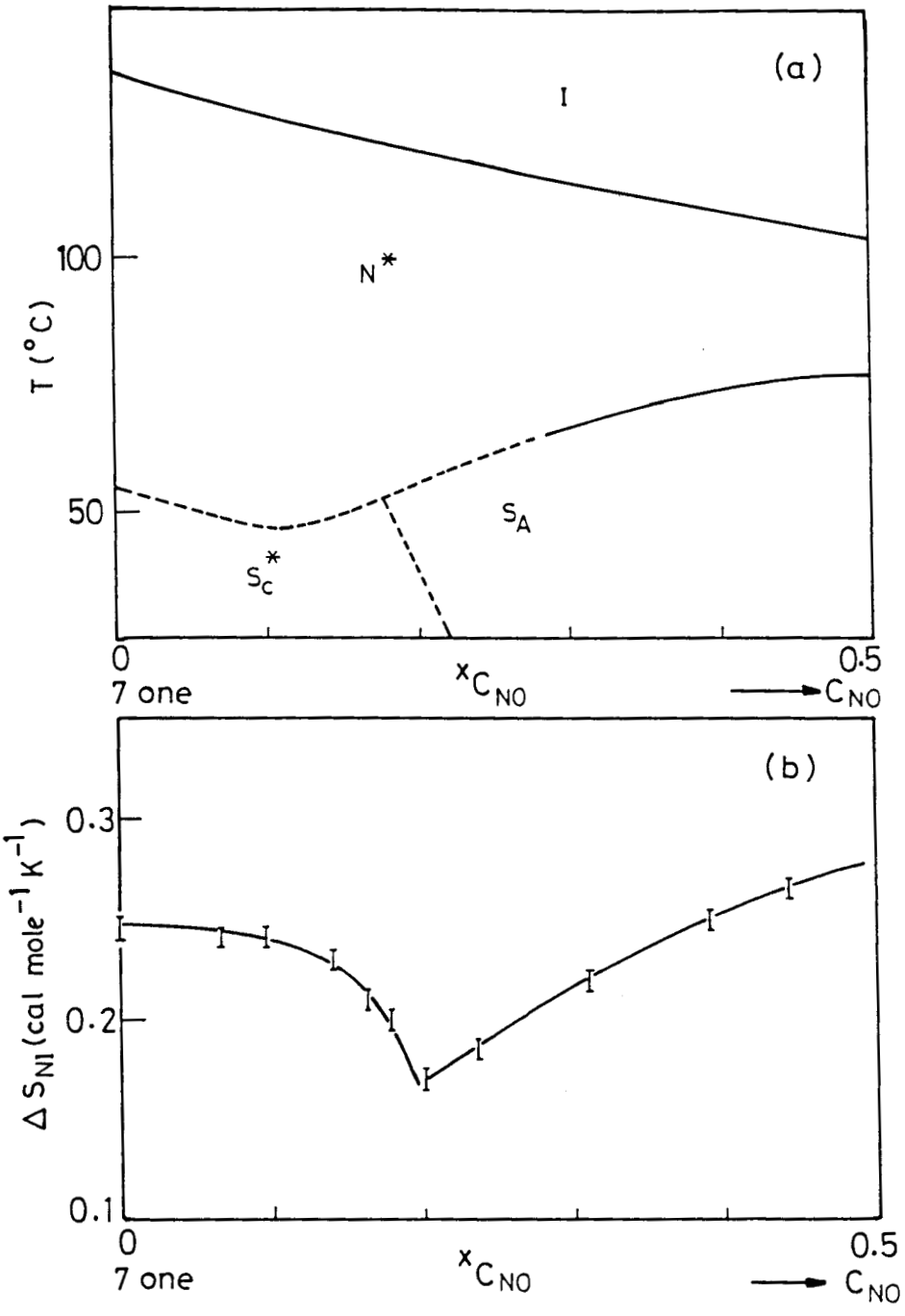

Figure 5.2

a) **Binary isobaric (1 bar) diagram between 70NE and C_{NO}**

b) **Variation of the nematic-isotropic transition entropy versus the molar fraction of C_{NO} in the mixture.**

* **indicates twisted nematic and chiral smectic C phases (ref. 5).**

4'-n-octyloxy-4-cyanobiphenyl (6OCB/8OCB), and, 80CB and 4-cyano-benzylidene-4'-octyloxy aniline (CBOOA). They found that a plot of (dT/dP) at 1 bar vs. concentration shows an anomalous decrease in the concentration range $0.1 < x < 0.28$, showing a minimum at a concentration where the range of smectic A phase is maximum. Their results are shown in Fig.5.3a and 5.3b. Volumetric studies by Guichard et al.[9] on mixtures of 8OCB/6OCB showed that the volume change (ΔV) at N-I transition for this system plotted as a function of concentration (X) shows an anomalous dip which is located at exactly the concentration at which Shashidhar et al.[6] observed a dip in the (dT/dP) vs. concentration plots. The ΔV vs. X plot of Guichard et al. is shown in Fig.5.4. Thus, these studies clearly showed that the thermodynamic properties of N-I transitions are influenced by coupling between nematic and smectic ordering.

Another evidence of the manifestation of the coupling between smectic and nematic ordering comes from a study of the pressure-temperature (P-T) diagrams of reentrant nematic systems. The P-T diagrams of several single component systems exhibiting re-entrant nematic phase showed[10-14] the following features:

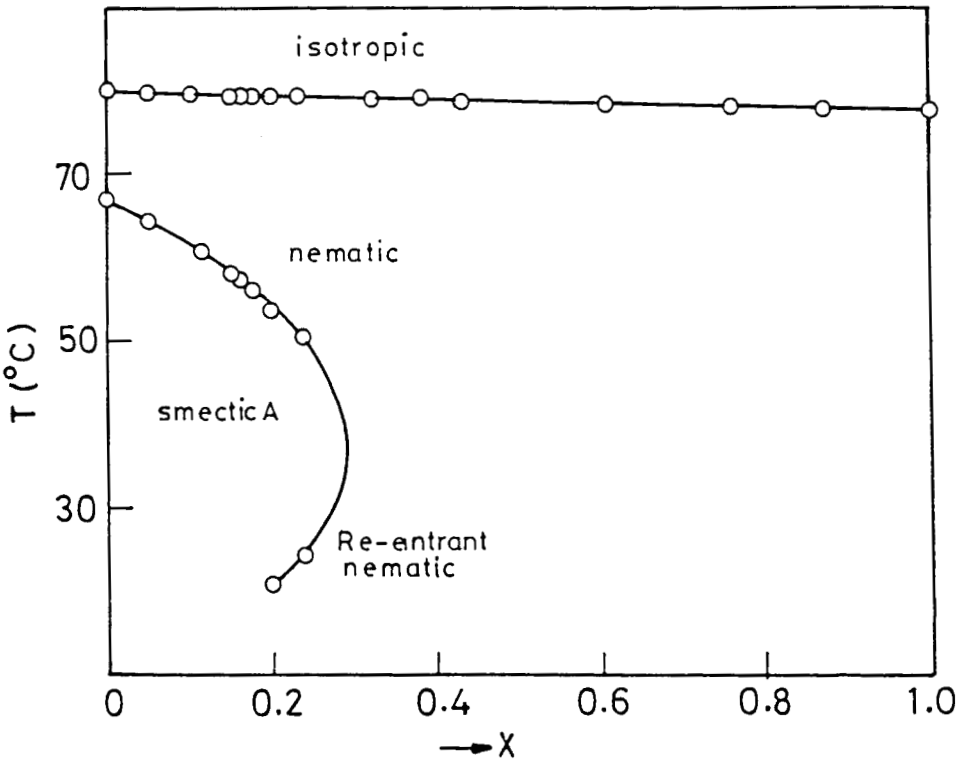

Figure 5.3(a)

Transition temperatures T at 1 bar in mixtures of 60CB and 80CB versus the mole fraction x of 60CB (Ref. 7).

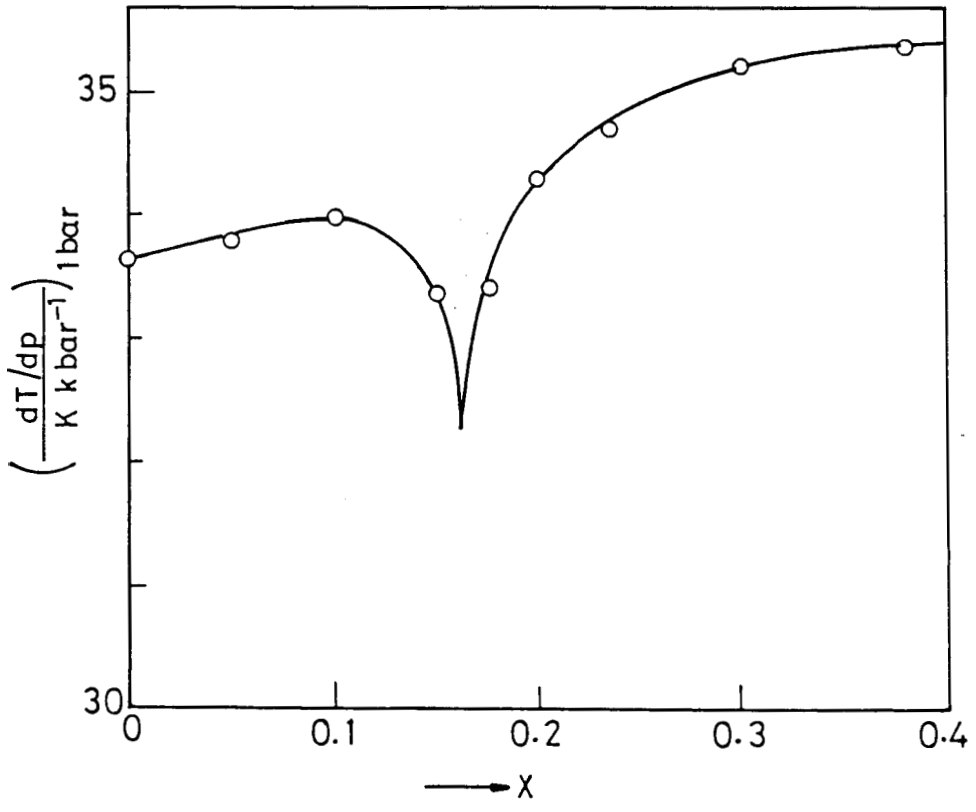

Figure 5.3(b)

$(dT/dP)_{,bar}$ values for the **N-I** transition in 60CB/80CB mixtures versus mole fraction x of 60CB as obtained from DTA (Ref.7).

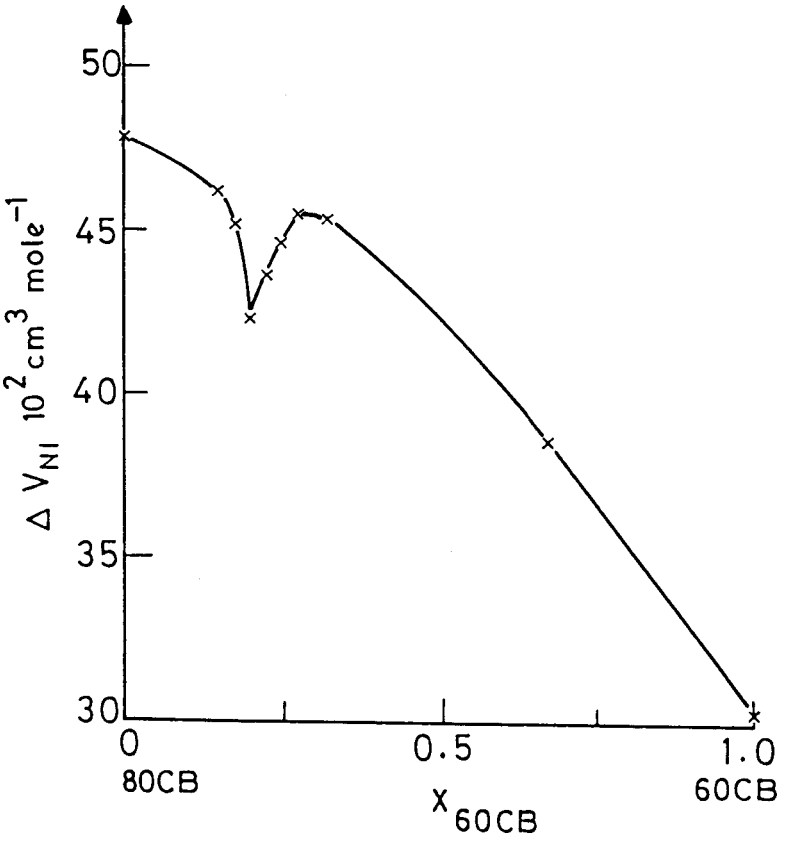

Figure 5.4

8OCB-6OCB **system : volume changes at the nematic-isotropic transition** (ref. **9**).

i) The nematic-smectic A phase boundary is elliptic in shape.

ii) There is a maximum pressure (P_m) beyond which the smectic A phase does not exist, and

iii) P_m is uniquely related to the range of the nematic phase at the atmospheric pressure.

Another important feature appeared to emerge from these phase diagrams. The major axis of the elliptically shaped nematic-smectic A phase boundary seemed to have the same slope as the N-I phase boundary which was a straight line. However this was not ascertained quantitatively. To investigate this point further, we have undertaken accurate mapping of the pressure-temperature diagrams of a number of single component systems. In addition, concentration-temperature diagrams of several binary liquid crystal systems exhibiting reentrant nematic phase at atmospheric pressure have also been obtained. The results of these studies which will be presented in this chapter show dramatically that the coupling between nematic and smectic ordering manifests in the phase diagrams exhibited by reentrant nematogenic systems.

Materials

The single component systems studied are:- (i) 4-cyanophenyl-3'-methyl-4'-(4"-n-undecyloxy-α-methylcinnamoyloxy)benzoate(11CPMαMCB), (ii) 4-cyanophenyl-3'-methoxy-4'-(4"-n-undecyloxy-α-methyl cinnamoy-

loxy) benzoate (11CPMeOαMCB), (iii) 4-cyanophenyl-3'-methyl-4'-(4"-n-undecylbenzoyloxy)benzoate (11CPMBB), and (iv) 4-cyanophenyl-3'-methyl-4'-(4"-n-dodecyloxy-α-methyl cinnamoyloxy) benzoate (12CPMαMCB), while the binary systems studied are CBOOA-CEPOOC,[15] CBOOA and 4-cyanoethylphenyl-4'-octyloxy benzoate (CEPOOB), 80CB and 4-n-octyloxybiphenyl-4'-cyanobenzoate (8OBCB),[16] and, CBOOA and 8OBCB. The chemical formulae of different materials are given in Fig. 5.5(a&b). The transition temperatures of the materials used in the pressure study are given in Table 5.1 while the transition temperatures of the compounds constituting the binary systems are listed in Table 5.2.

Results

The pressure-temperature diagrams have been obtained by the optical transmission technique described in chapter II. The precision in the determination of pressure is r2 bars and temperature is ±100 mK. The temperature-concentration diagrams were obtained by optical microscopic observation of the individual mixtures after ascertaining the homogeneity of the mixtures. The concentrations were determined to a precision of ±0.1%, while the transition temperatures were measured to a precision of ±100 mK. (The details of weighing, preparation of mixtures and determination of transition temperatures are discussed in section 3.2 of chapter III.)

We shall first discuss the results of our pressure studies for

80CB

4′– n– octyloxy–4– cyanobiphenyl

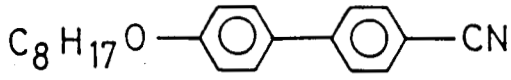

CBOOA

4– cyanobenzylidene – 4′–n–octyloxyaniline

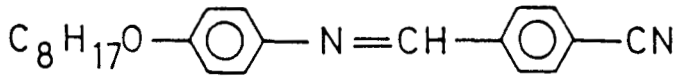

CEPOOB

4– cyanoethylphenyl–4′– octyloxybenzoate

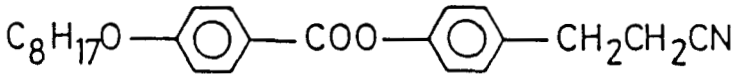

80BCB

4 –n– octyloxybiphenyl – 4′– cyanobenzoate

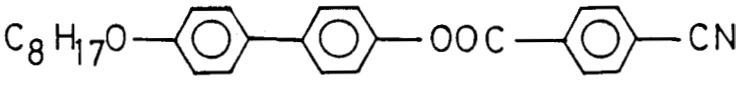

Figure 5.5(a)

Chemical structures of the compounds constituting the binary systems exhibiting the reentrant nematic behaviour.

1 11CPM αMCB

4 – cyanophenyl – 3′ – methyl – 4′ – (4″ – n – undecyloxy – α – methyl cinnamoyloxy) benzoate

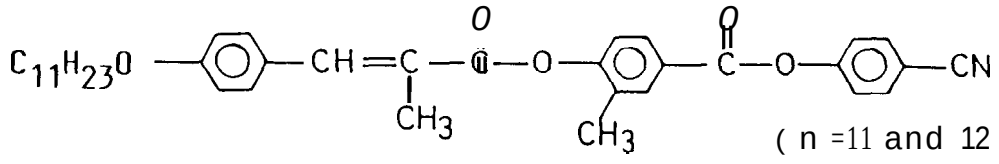

(n =11 and 12

2 11CPMeOαMCB

4 – cyanophenyl – 3′ – methyoxy – 4′ – (4″ – n – undecyloxy – α – methyl cinnamoyloxy) benzoate

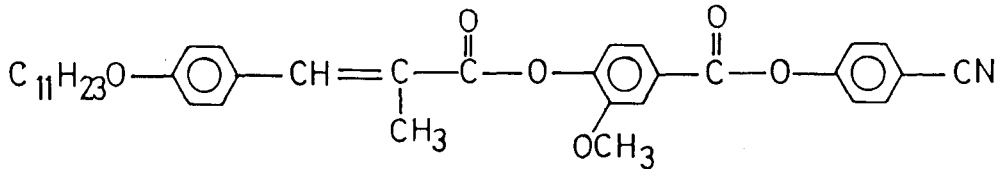

3 11 CPMBB

4 – cyanophenyl – 3′ – methyl – 4′ – (4″ – n – undecyloxy) benzoate

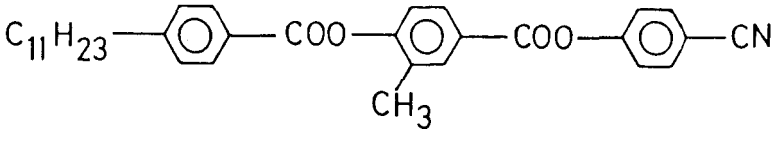

4 12 CPM α MCB

4 – cyanophenyl – 3′ – methyl – 4′ – (4″ n – dodecyloxy – α – methyl cinnamoyloxy) benzoate

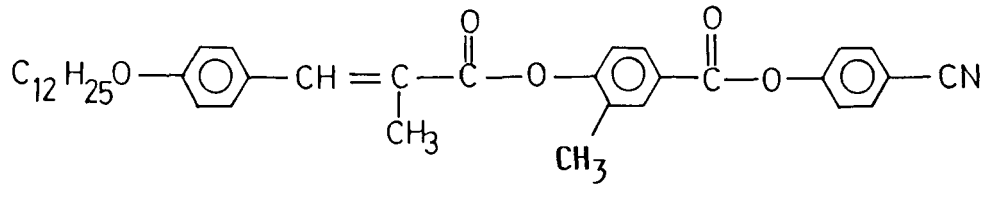

Figure 5.5b

The chemical structures of the single component systems chosen for pressure studies.

TABLE 5.1

Transition temperatures (in °C) of the single component systems used for P-T diagrams . .

Compound	K	RN	A	N	I
11CPMαMCB	78.2	96.0	126.8		167.9
11CPMeOαMCB	82.0	(51.0)	124.0		138.1
11CPMBB	103.0	(76.5)	126.30		150.3
12CPMαMCB	82	(69)	147.1		162.1

( ) denotes that the transition is monotropic

TABLE 5.2

Transition temperatures (in °C) of the materials used for temperature-concentration diagrams

Compound	K	C	S_A	N	I
CEPOOB	55.9	-	-	58	
CBOOA	73		82.5	107.2	
80CB	55		66.8	79.9	
8OBCB	127.8	(124.4)	159.4	234.3	

For transition temperatures of CEPOOC, see Table 3.3

( ) denotes the monotropic transition

four single component systems. The data are given in Figures 5.6-5.9. The features which are common to all the four compounds (as seen clearly from these P-T diagrams) are:

1 The smectic A phase is bounded in P-T plane with P_m as the maximum pressure up to which it exists,

2 the nematic-smectic A phase boundary is, as expected, elliptical in shape, and

3 the tilts of the major axis of the elliptical A-N boundary and the N-I line (which is straight) are the same.

We shall now quantitatively examine the slopes of the major axis of the elliptical A-N boundary and N-I line in the P-T plane.

Clark[17] and independently Klug and Whalley[18] analysed the shape as well as the thermodynamics of the smectic A-nematic phase boundary in the P-T plane. According to them the shape of the nematic-smectic A phase boundary may be quantitatively related to the thermodynamic parameters of the two phases by obtaining an expression for the pressure and temperature dependence of the difference in the Gibbs free energy (ΔG) between the nematic and smectic A phases, i.e., expressing AG in terms of P and T. In the vicinity of some reference point ($P_{o'}$ T_o), AG may be expressed in Taylor's series as

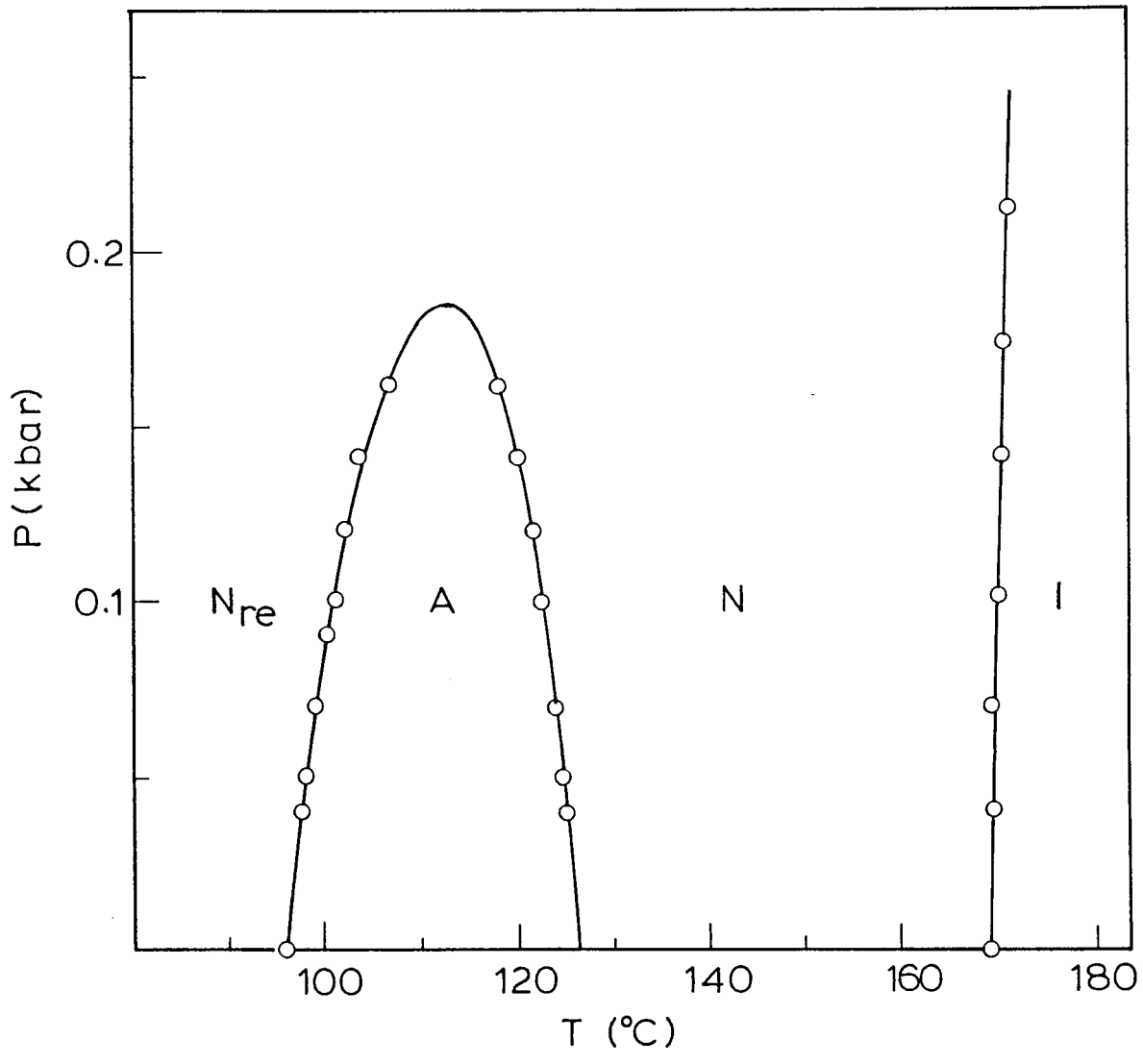

Figure 5.6

P-T diagram of 4-cyanophenyl-3'-methyl-4'-(4"-n-undecyloxy-α-**methyl cinnamoyloxy) benzoate. The open circles are data points while the solid lines are computer** fits **of the A-N and N-I data to the equations of an ellipse and a straight line respectively.**

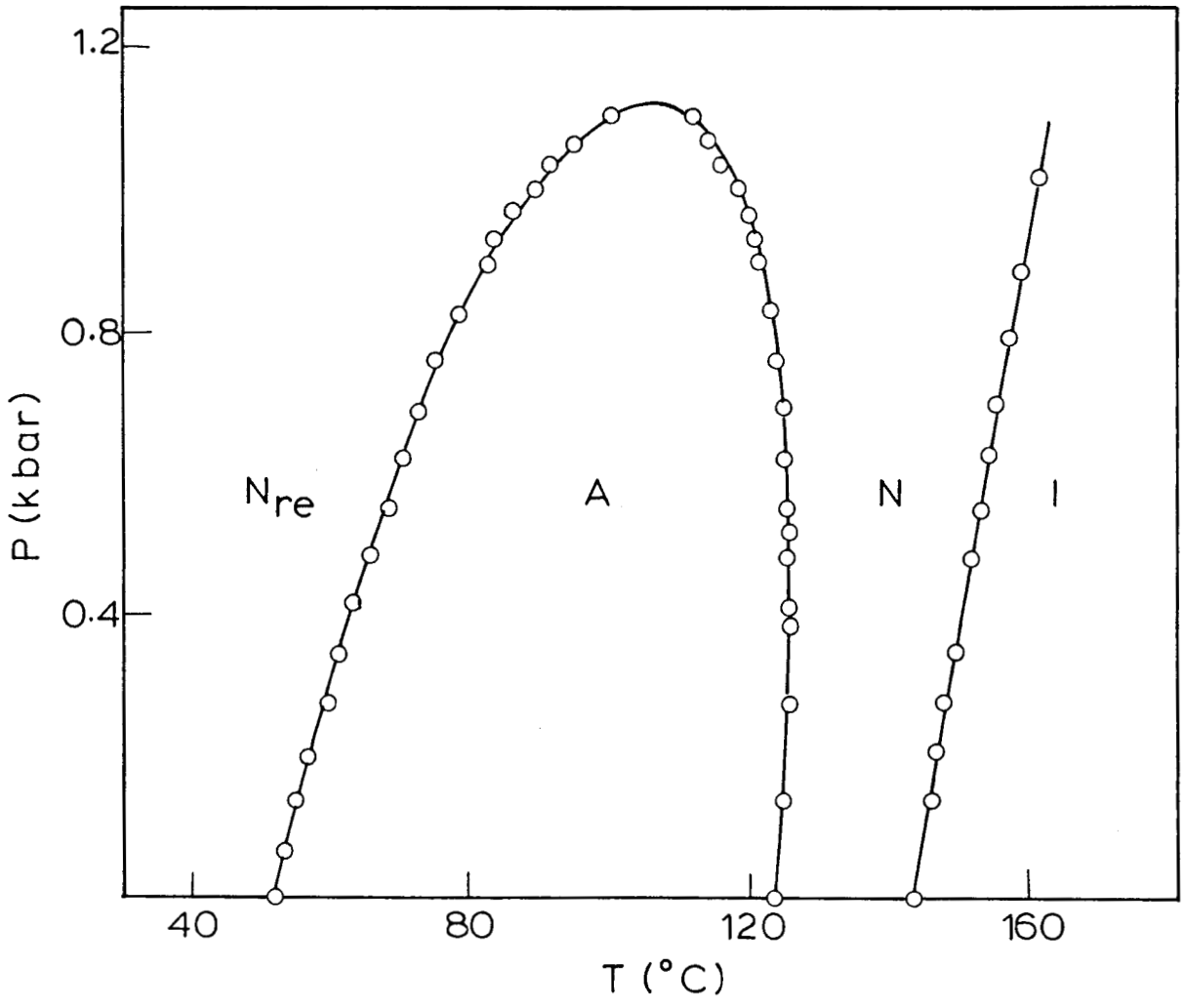

Figure 5.7

P-T diagram of 4-cynophenyl-3'-methoxy-4'-(4"-n-undecyloxy-α-methyl cinnamoyloxy) **benzoate (see also legend of figure 5.6).**

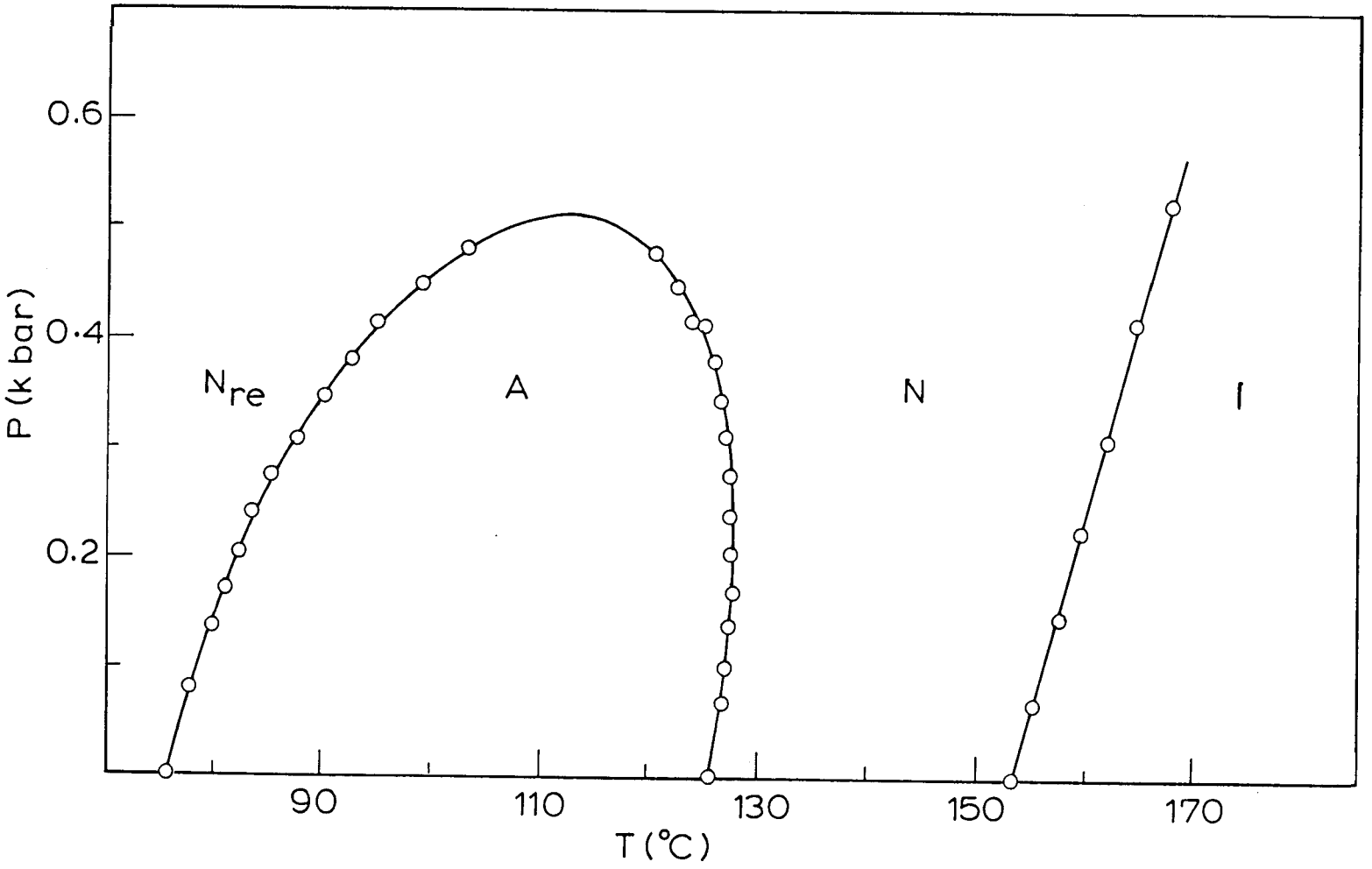

Figure 5.8

P-T diagram of 4-cyanophenyl-3'-methyl-4'-(4"-n-undecylbenzoyloxy) benzoate

(see also legend of 5.6).

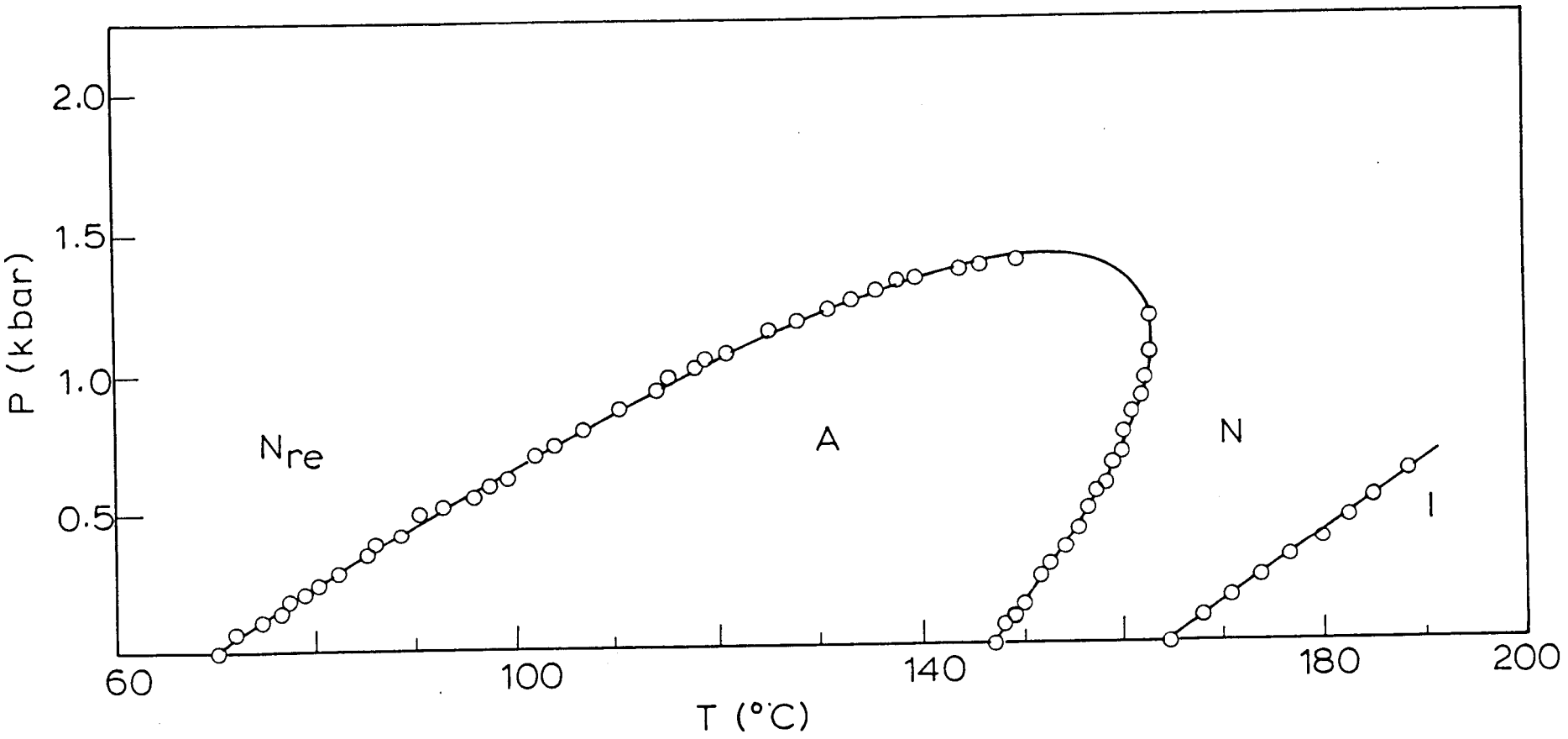

Figure 5.9

P-T diagram of 4-cyanophenyl-3'-methyl-4'-(4"-n-dodecyloxy-α-methyl cinnamoyloxy) benzoate

(see also legend of Fig. 5.6)

$$\Delta G = \Delta G_o + \Delta V_o (P - P_o) - \Delta S_o (T - T_o) + \frac{\Delta \beta}{2} (P - P_o)^2$$

$$+ \Delta \alpha (P - P_o)(T - T_o) - \frac{\Delta C_P}{2T_o} (T - T_o)^2 + \ldots \quad (1)$$

where the following notations are used -

$$\Delta G = G_N - G_A$$

$$\Delta S = S_N - S_A = -\left(\frac{\partial \Delta G}{\partial T}\right)_P$$

$$\Delta V = V_N - V_A = \left(\frac{\partial \Delta G}{\partial P}\right)_T \quad (2)$$

$$\Delta G_o = \Delta G(P_o, T_o)$$

$$\Delta S_o = \Delta S(P_o, T_o)$$

$$\Delta V_o = \Delta V(P_o, T_o)$$

$$\Delta \beta = \frac{\partial \Delta V}{\partial P}_T = \left(\frac{\partial \Delta V_N}{\partial P}\right) - \left(\frac{\partial V_A}{\partial P}\right)_T$$

$$\Delta \alpha = \left(\frac{\partial \Delta V}{\partial T}\right)_P = -\left(\frac{\partial \Delta S}{\partial P}\right)_T$$

$$\Delta C_P = T\left(\frac{\partial \Delta S}{\partial T}\right)_P$$

In the expression (1), the higher order terms have been neglected which implies that $\Delta\beta$, $\Delta\alpha$ and ΔC_P are assumed to be sufficiently independent of P and T over the range of pressures and temperatures under consideration here. It shall be seen later that this assumption is reasonable. The nematic-smectic A (NA) phase boundary in the

P-T plane is obtained from the equation (1) by setting AG to zero and solving for P(T). Expanding and rearranging equation (1), we have

$$aP^2 + cT^2 + bPT + dP + eT + f = 0 \qquad (3)$$

where $a = \frac{\Delta\beta}{2\Delta G_o}$

$$c = -\frac{\Delta C_P}{2T_o \Delta G_o}$$

$$b = \frac{\Delta\alpha}{\Delta G_o}$$

$$d = -\left(\frac{\Delta\beta}{\Delta G_o}\right) P_o - \left(\frac{\Delta\alpha}{\Delta G_o}\right) T_o = -2aP_o - bT_o \qquad (4)$$

$$e = \frac{\Delta C_P}{\Delta G_o} - \left(\frac{\Delta\alpha}{\Delta G_o}\right) P_o = -2cT_o - bP_o$$

$$f = 1 + \left(\frac{\Delta\beta}{2\Delta G_o}\right) P_o^2 + \left(\frac{\Delta\alpha}{\Delta G_o}\right) P_o T_o - \left(\frac{\Delta C_P}{2\Delta G_o}\right) T_o$$

$$= 1 + aP_o^2 + bP_o T_o + cT_o^2$$

Equation (3) is the general equation for a conic section. Thus P-T phase boundaries are at least locally expressible as conic sections and in systems, apparently like the ones under consideration, where ΔC_P, $\Delta\beta$ and $\Delta\alpha$ do not depend strongly on P and T, the phase boundary will have the shape of conic sections over a large area in the P-T plane. Elliptical phase boundaries will be obtained from equation (3) if,

$$\left| \frac{T_o \Delta\alpha^2}{\Delta\beta \Delta C_P} \right| < 1 \quad .$$

The fit of the A-N phase boundary data to equation (1) appears to involve varying of eight independent parameters, namely, $\Delta\beta$, P_o, $\Delta\alpha$, T_o, ΔC_P, AV_o, AS_o and AG_o. Since the choice of the reference point is arbitrary, Clark selected the reference point as the centre of the fitted ellipse. At this point ΔG_o is maximum and hence the first derivative of AG, namely, AV_o and AS_o are zero. This effectively eliminates four parameters P_o, T_o, ΔV_o and ΔS_o. The fitted ellipse will then be characterised by three quantities, the lengths of its major and minor axes, and θ_o, the angle of orientation of the major axis relative to the temperature axis. One is therefore left with three equations and four unknown quantities, viz., $\Delta\alpha$, $\Delta\beta$, ΔC_P and AG_o, and thus allowing the determination of ratios among any two of these four quantities. The fit of an ellipse to the data of Cladis et al.[10] is shown in Fig. 5.10 and it is excellent, which therefore, verifies the assumption that $\Delta\alpha$, $\Delta\beta$ and AC_P are reasonably constant over the area covered by the phase boundary in the P-T plane. This fit yields the following ratios :

$$\Delta\alpha/\Delta\beta = -0.7930 \text{ cal/sec x } °C$$

$$\Delta\beta/\Delta C_P = -0.019 \text{ CC}^2 \text{x} °C/\text{cal}^2$$

$$\Delta\alpha/\Delta C_P = 15.0 \times 10^{-3} \text{ CC/cal}$$

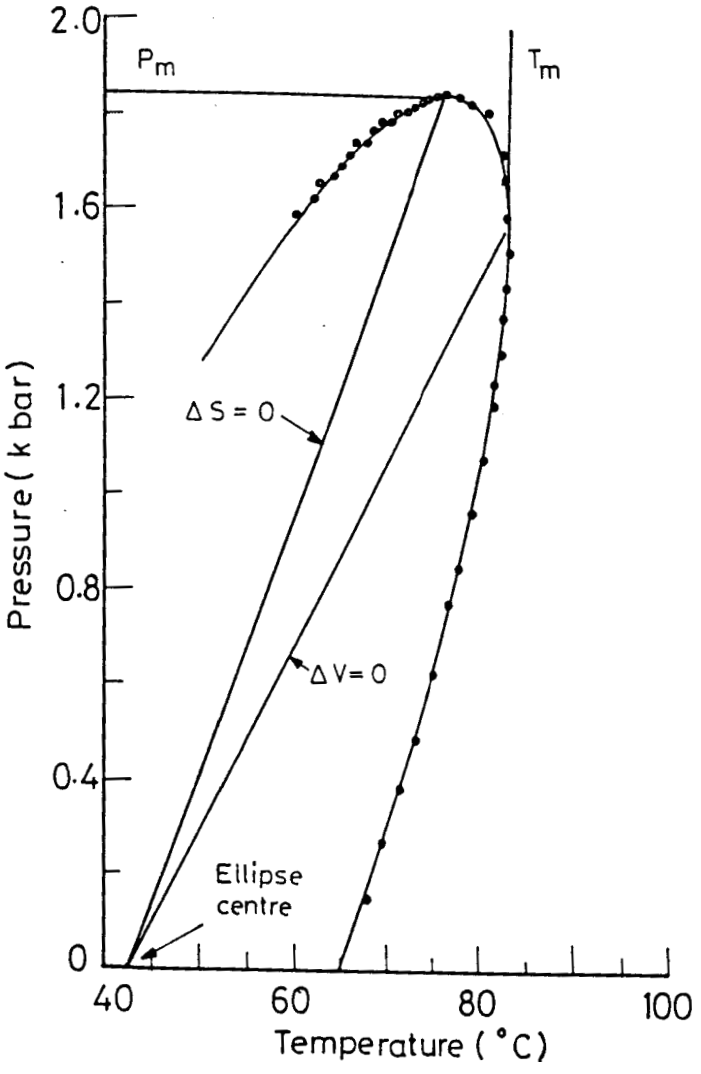

Figure 5.10

Smectic–nematic (AN) phase boundary of 8OCB. Solid curve represent; the best fit of an ellipse to the data of Cladis et al.[10] (after Clark[17]).

with P_o = 4.0 bars and T_o = 42.85°C, θ_o = 49.4' and

$$\left| \frac{\Delta \alpha^2 \, T_o}{\Delta \beta \Delta C_P} \right| = 0.51$$

while calculating the ratios, the following units have been used:

P (cal/cc), G (cal/mole), V (cc/mole),

S (cal/mole°C), α (cc/mole°C), β (cc^2/mole cal) and

C_p (cal/mole°C).

We shall discuss the results of our computations for the data given in Figures 5.6–5.9.

For the sake of simplicity of computation, we have reduced the number of constants in equation (3) by dividing throughout by f, so that equation (3) now reduces to the form

$$a'P^2 + b'PT + c'T^2 + d'P + e'T + 1 = 0 \qquad (5)$$

where a' = a/f, b' = b/f, c' = c/f and so on. The computations have been carried out by using a PDP-11 computer. The constants a', b', c', d' and e' evaluated by least-squares-fit of the data to equation (5) are given in Table 5.3. The fits of the data for elliptically shaped A-N boundary to the equation of an ellipse for the four systems studied by us are given in Figures 5.6–5.9, which have been drawn using Hewlett-Packard programmable calcuator with a plotter attachment.

TABLE 5.3

Constants evaluated from the fit of the experimental data of the A-N phase boundary to the Equation of an ellipse, (Eqn. 5) $a'P^2 + b'PT + c'T^2 + d'P + e'T + 1 = 0$

Sl. No.	Compound	Constants obtained from fit					P_o (kbars)	T_o (°C)
		a^1	b^1	c^1	d^1	e^1		
1	11CPMαMCB	0.066390	-0.0015631	0.0000824	0.02697096	-0.0183318	-0.8130618	103.48
2	11CPMeOαMCB	0.140154	-0.0050358	0.0001551	0.5073738	-0.3267644	-0.326764	82.564
3	11CPMBB	0.3371193	-0.005026	0.0001059	0.4904527	-0.02124	0.020658	100.8243
4	12CPMαMCB	0.1191633	-0.0062155	0.0000972	0.750240	-0.02109	-1.914875	47.28107

The open circles denote the data points while the solid curve represents the best-fit for the data points to the equation of an ellipse, i.e., the curve obtained by using the constants a', b', c', d' and e' listed in table 5.3. It is clear from the Figures 5.6-5.9 that the fits are indeed good. The inclination of the major axis of the elliptically shaped N-A boundary was calculated in each case using the equation,[18]

$$\tan 2\theta = \frac{b'r}{c'-r^2a'} \qquad (6)$$

where r is the ratio of unit lengths of pressure and temperature axes, a', b' and c' are the constants of the fit shown in table 5.3.

The nematic-isotropic phase boundary is a straight line and the data for the N-I boundary have been fitted to the equation of a straight line from which the slope of the N-I boundary, i.e., the tilt with respect to the temperature axis is calculated. The slopes for N-I lines thus calculated and the tilts of the major axis of elliptical shaped A-N boundary as calculated using equation *(6)* are listed in Table 5.4. It is clear from this table that the tilt of the major axis of elliptical phase boundary, within experimental errors, is the same as the tilt of the N-I boundary for each of the system.

Studies on Binary Mixtures

So far, we have seen the similarity of tilts of the major axis of the elliptical A-N phase boundary and N-I phase boundary which

TABLE *5.4*

Tilts of the major axis of elliptical AN phase boundary as calculated from Eqn. (6) and tilt of the N-I line as obtained from the fits to equation of a straight line

Sl.No.	Compound	tilt of major axis of A-N boundary θ_{major} (in deg.)	tilt of the N-I line θ_{N-I} (in deg.)
1	11CPMαMCB	88.5	88.4
2	11CPMeOαMCB	80.5	80.4
3	11CPMBB	73.3	74.0
4	12CPMαMCB	38.4	37.2

is linear. We shall see if this similarity is valid in temperature-concentration diagrams. We have studied phase diagrams of four binary systems consisting of materials of widely different chemical structure and hence widely different transition temperatures. The only common factor was that the materials possessed a strongly polar CN or NO_2 terminal group, so much so that the reentrant nematic phase is to be expected over a certain range of concentration. We present in Figures 5.11-5.14, the temperature-concentration diagrams of the four binary systems. It should be remarked here that the shape of the A-N phase boundary in the T-X plane has not been investigated earlier for many systems. In the case of 80CB-60CB mixtures it was concluded[19-21] that the A-N boundary is parabolic in the T-X plane. We have fitted our A-N data to the equation of an ellipse (eqn. 5) with X the concentration expressed as weight per cent replacing the pressure term P. The constants of the fit a', b', c', d', e' and the coordinates of the centre of the ellipse (X_o, T_o), obtained for each of the system are given in table 5.5. The fits of the T-X data for the A-N boundary to the equation of an ellipse and data of N-I transitions to an equation of a straight line are shown in Fig. 5.15a-d. The open circles are the data points whereas the solid line is the computer fit of the data to the equation (5). The slopes or tilts of the major axis of the elliptically shaped A-N boundary with the temperature axis, as calculated from eqn. *(6)* using the constants obtained from the fit (Table 5.5) are shown in the table 5.6. The

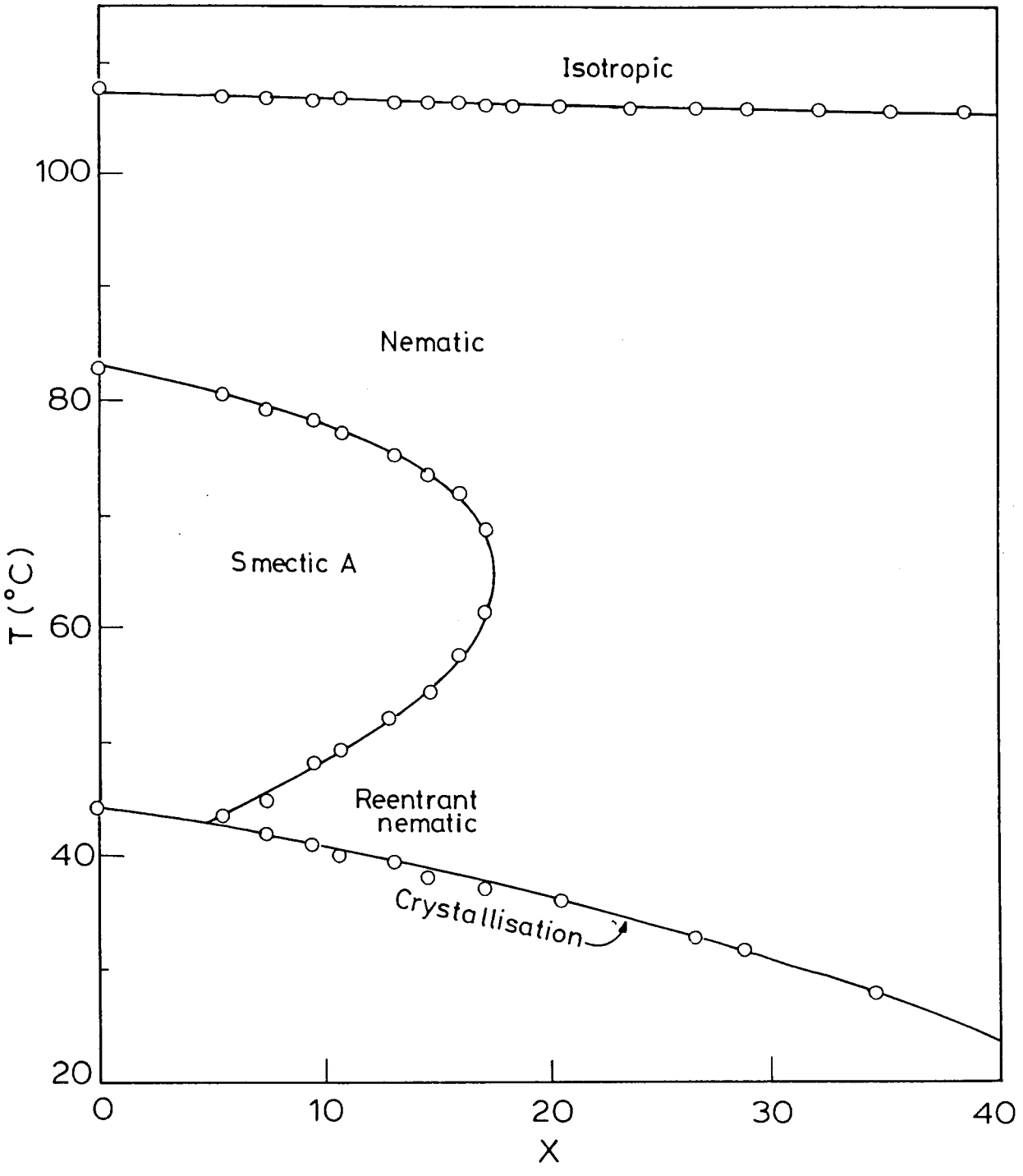

Figure 5.11

T-X diagram of binary mixtures of CBOOA and CEPOOC. X is the weight per cent of CEPOOC in the mixture.

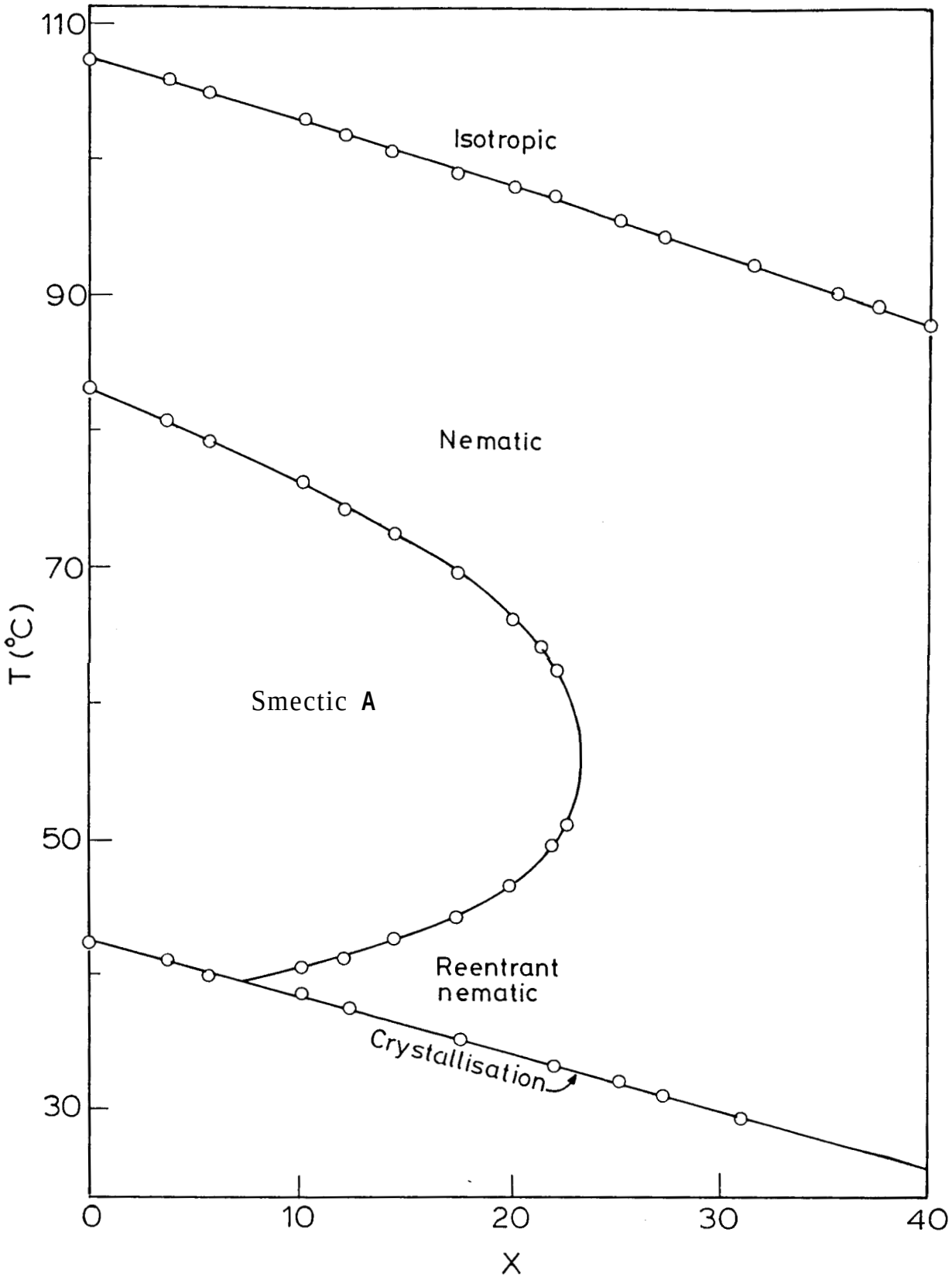

Figure 5.12

Temperature-concentration (T-X) diagram of binary mixtures of CBOOA and and CEPOOB. X is the weight per cent of CEPOOB in the mixture.

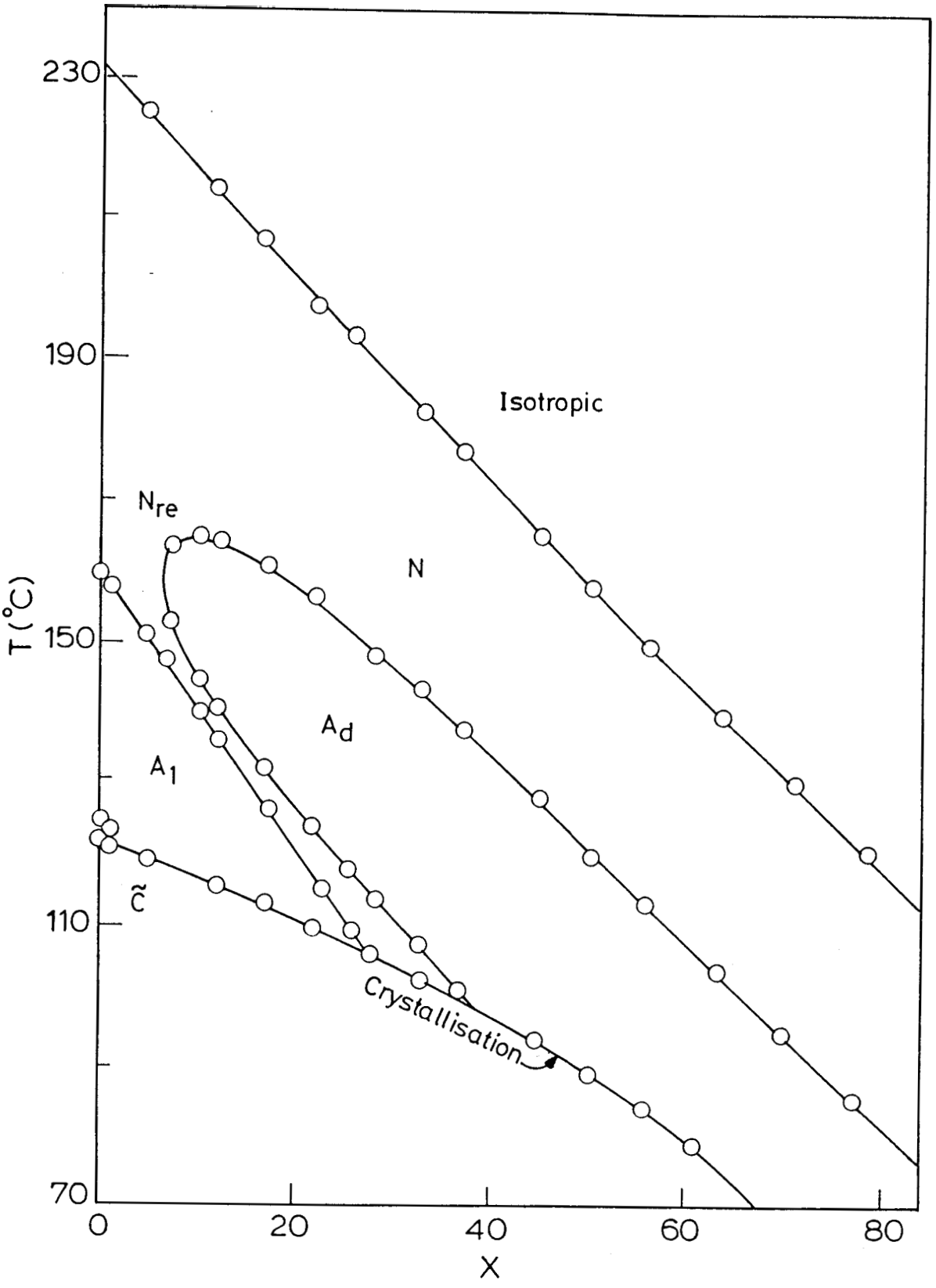

Figure 5.13

T-X diagram of binary mixtures 8OCB and 8OBCB. X is the weight per cent of 80CB in the mixture.

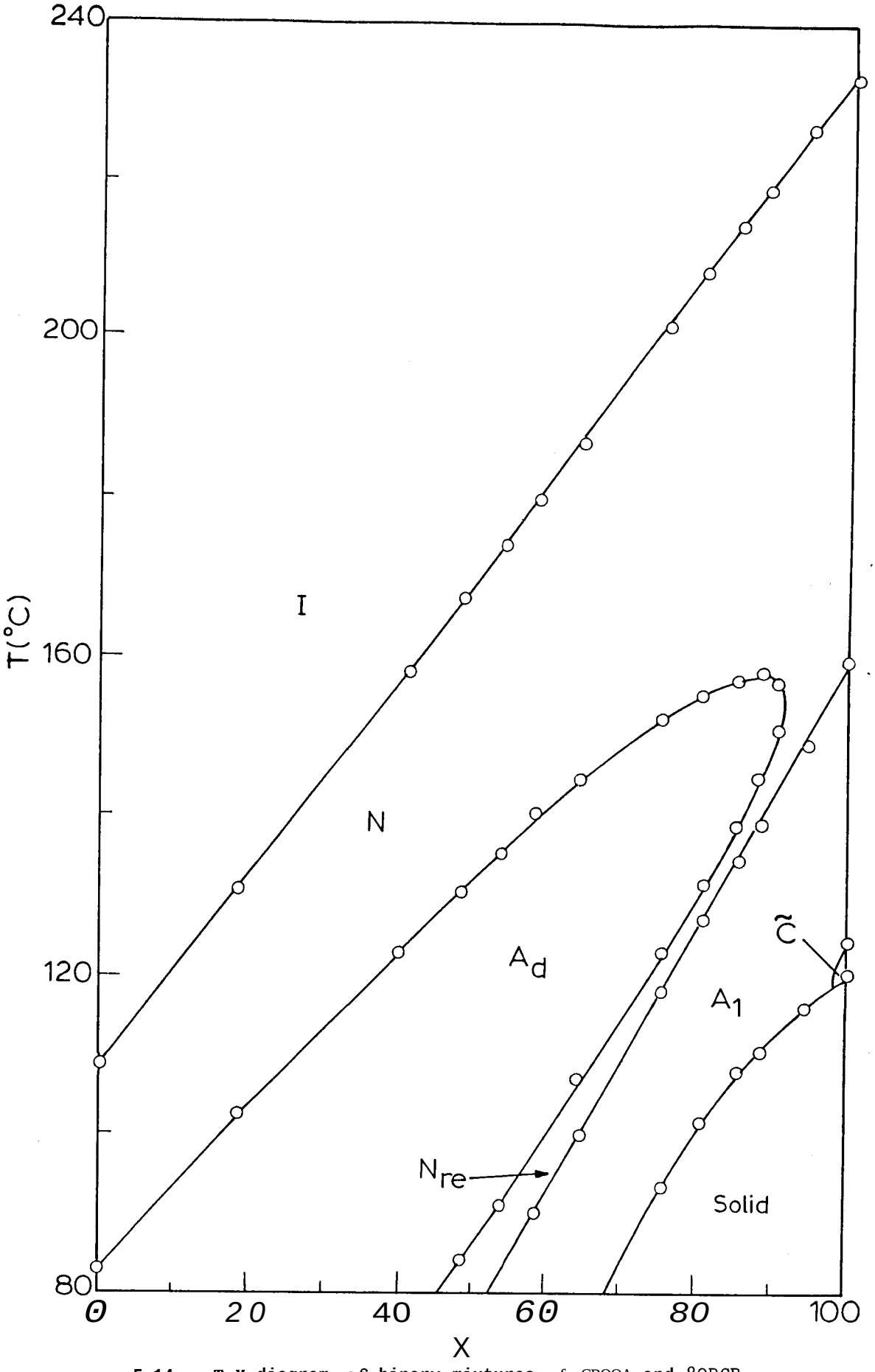

Figure 5.14 : T-X diagram of binary mixtures of CBOOA and 8OBCB. X is the weight per cent of 8OBCB in the mixture.

TABLE 5.5

Constants evaluated from the fit of the experimental A-N boundary data to the equation of an ellipse. (Equation 5, in which P is replaced by X the concentration)

Sl. No.	System	Constants from the fit					X_o	T_o (°C)
		a	b	c	d	e		
1	CBOOA/ CEPOOC (M_1)	0.0003319	-0.0000455	0.0002881	0.0033241	-0.0356684	61.83	-0.77
2	CBOOA/ CEPOOB (M_2)	0.0000659	0.0001189	0.000322	-0.0014396	-0.0387085	69.72	-52.02
3	8OCB/ 8OBCB (M_3)	-0.0408163	0.0549254	-0.0191127	-1.4049745	0.9748087	-117.89	-108.79
4	8OBCB/ CBOOA (M_4)	0.000626	-0.0010673	0.0004833	0.058757	-0.0521518	36.39	-15.92

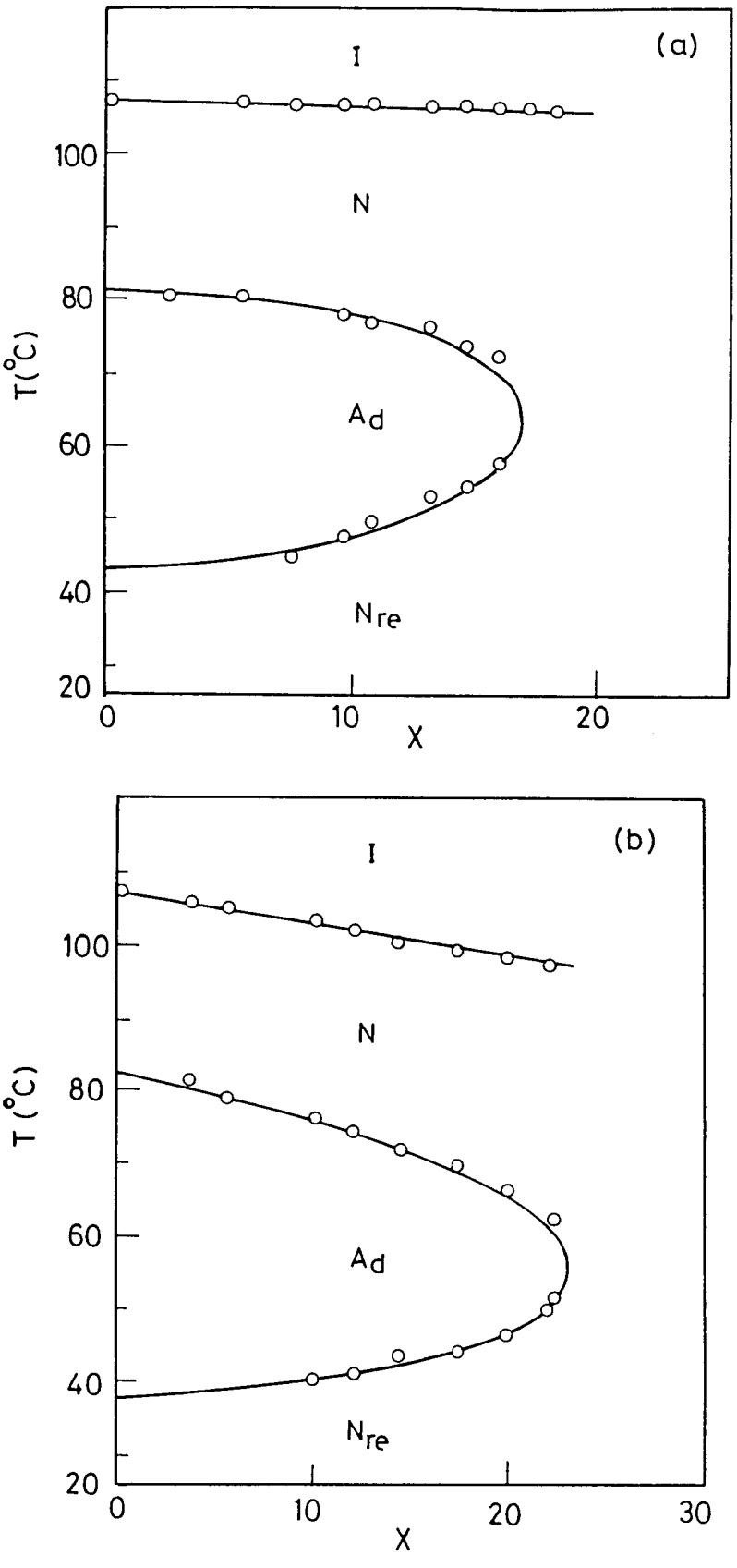

FIGURE 5.15

T–X diagrams for four binary systems showing the computer fits of the T–X data for the A–N and N–I transitions to the equation of an ellipse and a straight line respectively. The circles are the data points and the solid curves are obtained by computer fits (see text). The binary systems are (a) CBOOA/CEPOOC, (b) CBOOA/CEPOOB,

.....continued

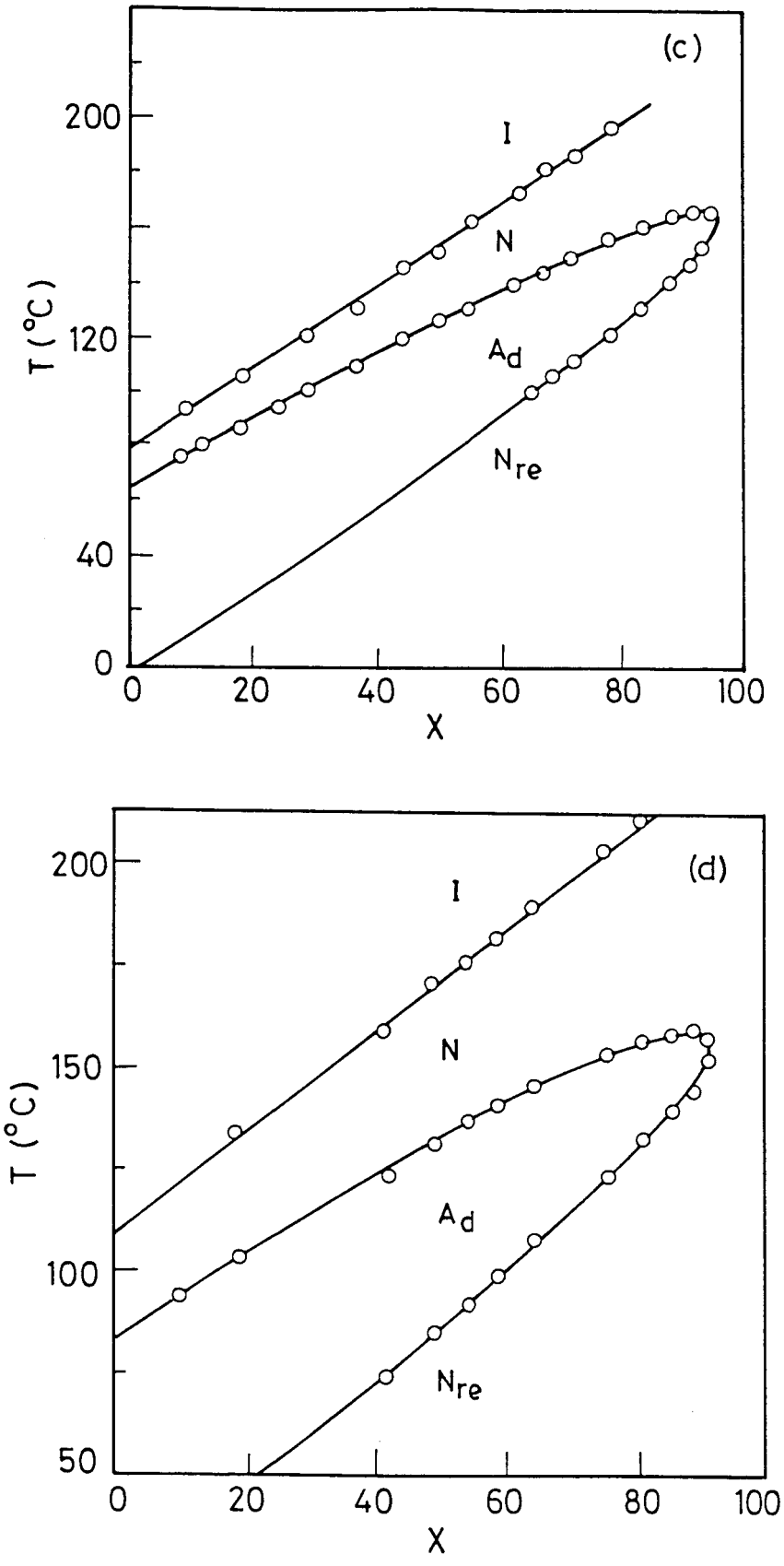

(c) 8OCB/8OBCB and (d) CBOOA/8OBCB. In every case X denotes the weight per cent of the second component.

TABLE 5.6

The tilts of the major axis of elliptically shaped A-N boundary as calculated from Eqn. (6) and the tilts of the N-I line obtained from the fits of N-I data to equation of a straight line.

Sl.No.	Binary system	Tilt of the major axis (in deg.) major axis	Tilt of the N-I boundary (in deg) N-I
1	CBOOA/CEPOOC (M1)	90.0	91.95
2	CBOOA/CEPOOB (M2)	96.0	98.00
3	8OCB/8OBCB (M3)	57.6	57.0
4	8OBCB/CBOOA (M4)	55.6	53.5

data for the N–I phase boundary which is a straight line were fitted to the equation of a straight line. The slopes of the N–I line obtained from the fit are also shown in Table 5.6. By comparing the slopes calculated for the major axis of the elliptical A–N phase boundary and the N–I phase boundary for each system, it is evident that within experimental errors, the tilts of the major axis and tilts of the N–I boundary are nearly the same for all the systems. Thus, it is clear that the major axis of the elliptically shaped A–N boundary is always parallel to the N–I line either in temperature–concentration plane or pressure–temperature plane, for any reentrant system regardless of (i) the material studied, (ii) the transition temperatures, and (iii) widely varying slopes of N–I boundary.

We have thus shown that the coupling between the smectic and nematic ordering is manifested in the phase diagrams of reentrant nematogens both in P–T and T–X planes. It is relevant to recall that recently Keyes[22] has developed a mean field theory for reentrant nematics by taking into account the coupling of smectic and nematic orders. By incorporating the lowest order coupling terms in the Landau free energy expansion, he has shown that observed features of the smectic A–nematic phase boundary come out as a consequence of this coupling. Exact comparisons between theory and experiments are yet to be worked out.

Gordetski and Podnek[23] have developed a model which permits

a unified description of the main types of liquid crystal phases as well as phase transitions between them. Their starting point was the fact that in liquid crystals generally there are two independent directions: one of them determines the orientational order of the nematic type and another gives the orientation of the smectic layers. The existence of these two directions means that a liquid crystal should be described by two order parameters, one of which is responsible for the formation of the nematic phase, the other for the smectic phases. The two tensor order parameters can be introduced either phenomenologically, or by separating the long-wave (nematic) and short-wave (smectic) components of a single tensor. This model describes a reentrant behaviour which is determined by competition between orientational and smectic ordering. The theoretical calculations of Gordetski et al. show that the disposition (slope) of the reentrant parabola should strongly depend on the slope of the N–I transition line. Our results clearly demonstrate that such a dependence is indeed seen experimentally.

REFERENCES

1 P.G.de Cennes, Solid State Commun., 10, 753 (1972); Mol.Cryst. Liquid.Cryst., 21, 49 (1973)

2 W.L.McMillan, Phys. Rev., **A6**, 936 (1972); **A** 7, 1673 (1972).

3 B.I.Halperin, T.C.Lubensky and S.Ma, Phys. Rev. Lett., 32, 292 (1974)

4 B.I.Halperin and T.C.Lubensky, Solid State Commun., 14, 997 (1974)

5 M.F.Achard, G.Sigaud, F.Hardouin, "Liquid Crystals of One- and Two-Dimensional Order", Eds. W.Helfrich and G.Heppke (Springer-Verlag, Berlin, 1980), p. 149

6 R.Shashidhar, H.D.Kleinhans and G.M.Schneider, Mol. Cryst. Liq. Cryst. Lett., 72, 119 (1981)

7 H.D.Kleinhans, R.Shashidhar and G.M.Schneider, Mol. Cryst. Liq. Cryst. Lett., 82, 19 (1982)

8 H.D.Kleinhans, G.M.Schneider and R.Shashidhar, Mol. Cryst. Liq. Cryst., 103, 255 (1983)

9 Y.Guichard, G.Sigaud and F.Hardouin, Mol. Cryst. Liq. Cryst. Lett., 102, 325 (1984)

10 P.E.Cladis, R.K.Bogardus, W.B.Daniels and G.N.Taylor, Phys. Rev. Lett., 39, 720 (1977)

P.E.Cladis, R.K.Bogardus and D.Aadsen, Phys. Rev., **A18**, 2292 (1978)

J.Hermann, Mol. Cryst. Liq. Cryst. Lett., 72, 219 (1982)

A.N.Kalkura, R.Shashidhar and N.Subramanya Raj Urs, J. de Phys., 44, 51 (1983)

S.Krishna Prasad, S.Pfeiffer, G.Heppke and R.Shashidhar, Z. Naturforsch., **40a**, 632 (1985)

15 G.Pelzl, S. Diele, A. Weigeleben and D. Demus, Mol. Cryst.Liq.Cryst. Lett., 64, 163 (1981)

16 J.W.Goodby and C.R.Walton, Mol. Cryst. Liq. Cryst., 122, 219 (1985)

17 N.A.Clark, J. de Phys., 40, C3-345 (1979)

18 D.D.Klug and E.Whalley, J. Chem.Phys., 71, 1874 (1979)

19 P.S.Pershan and J.Prost, J.de Phys. Lett., 40, L-27 (1979); see also P.E.Cladis, Phys. Rev. Lett., **39**, 720 (1977)

20 A.R.Kortran, H.Von Kanel, R.J.Birgeneau and J.D.Litster, Phys. Rev. Lett., 47, 1206 (1981)

21 A.R.Kortran, H.Von Kanel, R.J.Birgeneau and J.D.Litster, J. de Phys., 45, 529 (1984)

22 P.H.Keyes, Presented at the Tenth International Liquid Crystal Conf., York, July 1984.

23 E.E.Gordetskii and V.E.Podnek, Sov. Phys. Crystallogr., 29, 618 (1984)